Robust Recursive Eigendecomposition and Subspace-Based Algorithms With Application to Fault Detection in Wireless Sensor Networks

S. C. Chan, *Member, IEEE*, H. C. Wu, and K. M. Tsui

***Abstract*—The principal component analysis (PCA) is a valuable tool in multivariate statistics, and it is an effective method for fault detection in wireless sensor networks (WSNs) and other related applications. However, its online implementation requires the computation of eigendecomposition (ED) or singular value decomposition. To reduce the arithmetic complexity, we propose an efficient fault detection approach using the subspace tracking concept. In particular, two new robust subspace tracking algorithms are developed, namely, the robust orthonormal projection approximation subspace tracking (OPAST) with rank-1 modification and the robust OPAST with deflation. Both methods rely on robust M-estimate-based recursive covariance estimate to improve the robustness against the effect of faulty samples, and they offer different tradeoff between fault detection accuracy and arithmetic complexity. Since only the ED in the major subspace is computed, their arithmetic complexities are much lower than those of other conventional PCA-based algorithms. Furthermore, we propose new robust T^2 score and SPE detection criteria with recursive update formulas to improve the robustness over their conventional counterparts and to facilitate online implementation for the proposed robust subspace ED and tracking algorithms. Computer simulation and experimental results on WSN data show that the proposed fault detection approach, which combines the aforementioned robust subspace tracking algorithms with the robust detection criteria, is able to achieve better performance than other conventional approaches. Hence, it serves as an attractive alternative to other conventional approaches to fault detection in WSNs and other related applications because of its low complexity, efficient recursive implementation, and good performance.**

***Index Terms*—Fault detection, orthonormal projection approximation subspace tracking (PAST) (OPAST), outlier detection, PAST algorithm with deflation (PASTd), recursive principal component analysis (R-PCA), robust statistics, subspace eigendecomposition (ED), wireless sensor networks (WSNs).**

I. Introduction

A WIRELESS sensor network (WSN) is a network made up of a large number of sensor nodes distributed in a large area for monitoring physical variables such as temperature, humidity, voltage, etc. Typical applications of WSNs include environmental and habitat monitoring [1], health and medical monitoring, surveillance [2], irrigation systems [3], industrial monitoring [4], and so on. To maintain the reliability of a WSN, outlier detection is necessary to facilitate appropriate human intervention for fixing potential physical hazards due to abnormal observations or measurements collected by the sensor nodes. The occurrence of faulty samples can be caused by internal and external factors [5]. Internal factors refer to hardware failure, such as errors generated due to low battery power [6], while external factors refer to physical events such as a sudden rise of temperature caused by chemical fire and a sudden increase in network traffic due to malicious attack on the network.

In [7], a histogram-based approach has been proposed to detect faulty samples in WSNs. Since the histogram information is partially updated when major network changes are detected, it is amendable to online implementation. Moreover, during data exchange between sensor nodes, its low communication overhead leads to an advantage of reduced energy consumption. This will increase the life-span of sensor nodes. However, this approach only focuses on the analysis of single physical variable. Very often, multiple physical variables should be monitored simultaneously.

For fault detection with multiple physical variables, the measurement variables are usually correlated, for example, the dependence between the resistance of a wire and surrounding temperature. Moreover, the WSN can be regarded as a time-variant system, where the measurement variables are time varying due to environmental changes such as the variation of light intensity between day time and night time. To handle such correlated measurement variables, multivariate statistical processing methods such as the principal component (PC) analysis (PCA) and the partial least squares can be used [8]. Among these two methods, the PCA is commonly adopted [9]–[11] because of its robustness and reliability [8].

The usefulness of PCA for fault detection in WSNs was first reported in [9]. It is able to capture the dependence of the measurement variables and detect correlated faults or anomalies that span through multiple groups of sensor nodes. One major limitation of the conventional PCA approach is that it does not support real-time monitoring of possible system changes, for example, due to temperature variation. To overcome this limitation, the exponentially weighted PCA (EWM-PCA) [12], [13] and the recursive PCA (R-PCA) [14] have been developed for process monitoring. They support real-time monitoring and

Manuscript received April 4, 2011; revised August 4, 2011; accepted September 28, 2011. Date of publication February 22, 2012; date of current version May 11, 2012. The Associate Editor coordinating the review process for this paper was Dr. Maciej Zawodniok.

The authors are with the Department of Electrical and Electronic Engineering, The University of Hong Kong, Pokfulam, Hong Kong.

Color versions of one or more of the figures in this paper are available online at http://ieeexplore.ieee.org.

Digital Object Identifier 10.1109/TIM.2012.2186654

are more adaptive to system changes. While the EWM-PCA has high implementation complexity due to the expensive eigendecomposition (ED) and singular value decomposition (SVD), the R-PCA is very efficient in computing recursively the ED by means of two rank-1 modifications. However, all the aforementioned algorithms still require the explicit computation of all associated eigenvectors and eigenvalues of the entire ED.

In this paper, we propose an efficient online fault detection approach with reduced arithmetic complexity based on recursive subspace tracking concept [15]–[21], such as the orthonormal projection approximation subspace tracking (PAST) (OPAST) algorithm. Its main advantage is that only the major subspace is recursively tracked in order to compute the associated eigenvector and eigenvalues for fault detection. In particular, after the subspace and associated components have been tracked, major eigenvectors and eigenvalues in the subspace required by the fault detection algorithm can be computed by either rank-1 modification or deflation. This results in two new algorithms, namely, the OPAST with rank-1 modification (OPASTr) and the OPAST with deflation (OPASTd), which offer a tradeoff between the accuracy in identifying the faults and arithmetic complexity. The new algorithms can also be viewed as an extension of the conventional OPAST algorithm for computing eigenvectors and eigenvalues in the subspace.[1] Since the proposed algorithms only work on the major signal subspaces with a much smaller dimension, the arithmetic complexities are much lower than computing the whole ED using PCA-based algorithms such as the EWM-PCA and R-PCA.

Another objective of this paper is to improve the robustness of the proposed algorithms against the outliers or faulty samples. The resultant algorithms are called robust OPASTr (R-OPASTr) and robust OPASTd (R-OPASTd) algorithms. Faulty samples may mask subsequent faults if they are used to update the PCA model [8]. To suppress such effect, either the samples should be removed or their subsequent masking effects should be estimated and compensated, once they are identified as undesired outliers. In this paper, the concept of outlier removal is incorporated in the proposed algorithms by means of robust M-estimation of the recursive covariance estimate [22], which is useful in removing or suppressing the contribution of the faulty samples to the subspace estimation. Moreover, the recursive covariance update formula leads to an efficient online implementation of the proposed algorithms, which, in turn, are able to adapt to possible system changes.

Similarly, we extend the conventional T^2 score and squared prediction error (SPE) detection criteria using the concept of robust M-estimation [23]. To facilitate online implementation, we also develop recursive update formulas for these detection criteria based on the robust z-score reported in [24]. The resultant robust T^2 score and robust SPE offer better robustness over their conventional counterparts under the presence of faulty samples or outliers. Also, simulation and experimental results show that they can improve the performance of the conventional PCA-based fault detection algorithms. Overall, the proposed fault detection approach, which combines the aforementioned robust subspace tracking algorithms with the robust detection criteria, is able to achieve better performance than other conventional approaches. Its low complexity, efficient recursive implementation, and good performance make it as an attractive alternative to other conventional approaches used in WSNs and other related applications.

This paper is organized as follows: The background of WSNs and conventional fault detection algorithms and criteria are introduced in Section II. In Section III, the proposed robust fault detection approach, including new robust subspace tracking algorithms and fault detection criteria, is discussed. Design examples and comparisons with conventional algorithms are presented in Section IV. Finally, conclusions are drawn in Section V.

II. Background

In a WSN, the two most popular methods for performing outlier detection are the centralized approach and the distributed approach. In the centralized approach, raw measurements obtained from all sensor nodes are sent to the sink for outlier detection. Very often, the sink has the knowledge of overall network topology and collects the measurements from all associated sensor nodes in the WSN. In a large-scale environment, the centralized approach requires high communication overhead which leads to high energy consumption. On the other hand, in the distributed approach, outlier detection is performed at each sensor node by local outlier detection algorithm. Comparing with the centralized approach, the distributive approach is preferred as more in-network computation is performed and only important information is exchanged among the sensor nodes. Therefore, the communication overhead and energy consumption are significantly reduced.

A sensor fault is often referred to as an abnormal behavior of a sensor in WSNs. When a fault is developed in a sensor, the measurements deviate considerably from those measured in normal operation, which are also called the outliers. The following two types of faulty readings are often observed in the sensors deployed in WSNs.

1) Impulsive fault: an impulsive and abrupt change in measured value between two successive samples. For example, in [1], impulsive faults were found in sensors with occasional short circuit created between the positive and negative terminals of the Bayonet Neill–Concelman connectors due to the moisture of mud.
2) Mean-shift fault: constant offset readings of the sensor possibly caused by improper calibration and missing data as mentioned in [25].

In this paper, we focus on the detection of impulsive faults, which can also be extended to the detection of mean-shift fault with the aid of wavelet transform [26], [27]. More precisely, by transforming the data into the wavelet domain, the mean-shift fault can be represented in the wavelet coefficients with two impulses indicating the beginning and the end of the mean-shift fault. Therefore, the detection of mean-shift fault in the time domain can be reformulated as the detection of impulsive fault in the wavelet domain. As a result, the mean-shift fault can be

[1] When applying the OPAST algorithm in array signal processing, the explicit computation of eigenvectors and eigenvalues in the tracked subspace is not required.

identified by detecting the impulses in the wavelet domain using the proposed fault detection algorithm. Interested readers are referred to [26] and [27] for mean-shift detection using wavelet transform.

A. Conventional Fault Detection Algorithms

A commonly used local fault detection technique is the PCA. Its main idea is to first project the measurement vectors into the signal subspace spanned by a number of chosen major PCs and then identify outliers in the signal subspace. More precisely, consider a Pth variable vector $\boldsymbol{x} = [x_1, x_2, \ldots, x_P]^{\mathrm{T}}$, where the superscript T denotes matrix transposition. We are given N measurements of $\boldsymbol{x}$, where $\boldsymbol{x}_i = [x_{i,1}, x_{i,2}, \ldots, x_{i,P}]^{\mathrm{T}}$, $i = 1, \ldots, N$, is the ith measurement vector obtained, for example, at a certain time instant i. $\boldsymbol{x}_i$ is usually "centered," i.e., with its mean removed, before the PCs are computed. Hence, the mean of $\boldsymbol{x}_i$, $i = 1, \ldots, N$, is first computed and is subtracted from each of the measurement vector to form $\overline{\boldsymbol{x}}_i$. Let $\boldsymbol{X} = [\overline{\boldsymbol{x}}_1, \overline{\boldsymbol{x}}_2, \ldots, \overline{\boldsymbol{x}}_N]^{\mathrm{T}}$ be the data matrix after centering. In PCA, we wish to express the centered random vector $\overline{\boldsymbol{x}}$ in terms of B PCs

$$\overline{\boldsymbol{x}} = \sum_{m=1}^{B} t_m \boldsymbol{p}_m + \boldsymbol{e} \tag{1}$$

where B is an appropriately chosen number of PCs to achieve a sufficiently small approximation error $\boldsymbol{e}$, $\boldsymbol{p}_m$ is the mth PC, and t_m is its associated score. Using (1), $\boldsymbol{X}$ can be written as

$$\boldsymbol{X} = \sum_{m=1}^{B} \boldsymbol{t}_m \boldsymbol{p}_m^T + \boldsymbol{E} = \boldsymbol{\Gamma} \boldsymbol{P}^T + \boldsymbol{E} \tag{2}$$

where $\boldsymbol{\Gamma} = [\boldsymbol{t}_1, \ldots, \boldsymbol{t}_B]$ is the score matrix, $\boldsymbol{t}_m = [t_{m,1}, \ldots, t_{m,N}]^{\mathrm{T}}$, $t_{m,i}$ is the associated score for the ith measurement vector, $i = 1, \ldots, N$, $\boldsymbol{P} = [\boldsymbol{p}_1, \ldots, \boldsymbol{p}_B]^{\mathrm{T}}$ is the collection of PCs or loading matrix, and $\boldsymbol{E}$ is the error matrix. A common way to determine the PCs is to compute the ED of the empirical correlation matrix

$$\boldsymbol{C}_{\boldsymbol{xx}} = E[\overline{\boldsymbol{x}} \cdot \overline{\boldsymbol{x}}^T] = \frac{1}{n-1} \boldsymbol{X}^T \boldsymbol{X} = \boldsymbol{U} \Lambda \boldsymbol{U}^T \tag{3}$$

where the columns of $\boldsymbol{U}$ are the eigenvectors and they are also the PCs and $\boldsymbol{\Lambda} = \mathrm{diag}\{\lambda_1, \ldots, \lambda_P\}$ contains the eigenvalues in descending order of magnitude $(\lambda_1 \geq \lambda_2, \ldots, \geq \lambda_P)$. If the first B largest eigenvalues and their eigenvectors $\boldsymbol{U}_B$ are retained, then one gets $\boldsymbol{P} = \boldsymbol{U}_{\boldsymbol{B}}$. The subspace spanned by the major PCs $\boldsymbol{P} = \boldsymbol{U}_{\boldsymbol{B}}$ is usually referred to as the signal subspace. The estimate $\hat{\boldsymbol{X}}$ is

$$\hat{\boldsymbol{X}} = \boldsymbol{X} \left(\boldsymbol{U}_B \boldsymbol{U}_B^T \right) = \boldsymbol{\Gamma} \boldsymbol{P}^T. \tag{4}$$

Comparing (2) with (4) above, one finds $\boldsymbol{\Gamma} = \boldsymbol{X} \boldsymbol{U}_B$. Alternatively, the PCs can also be computed from the SVD of the data matrix $\boldsymbol{X}$ as $\boldsymbol{X} = \boldsymbol{V} \boldsymbol{\Lambda}^{1/2} \boldsymbol{U}^T$, where $\boldsymbol{V}$ and $\boldsymbol{U}$ are orthogonal matrices and $\boldsymbol{\Lambda}^{1/2}$ is a diagonal matrix containing the singular values. The corresponding estimate $\hat{\boldsymbol{X}} = (\boldsymbol{V}_B \boldsymbol{\Lambda}_B^{1/2}) \boldsymbol{U}_B^T$ can be similarly found by retaining the first B largest singular values, and hence, the score matrix is $\boldsymbol{\Gamma} = \boldsymbol{V}_B \boldsymbol{\Lambda}_B^{1/2}$. For simplicity, only the ED in (3) is considered in this paper. The residual $\boldsymbol{E}$ in (2) can be found by subtracting the estimate $\hat{\boldsymbol{X}}$ from the original data matrix $\boldsymbol{X}$, i.e., $\boldsymbol{E} = \boldsymbol{X} - \hat{\boldsymbol{X}}$. For online applications, $\boldsymbol{x}$ may be taken over consecutive time instants. Denote the corresponding sample at the time instant t by $\boldsymbol{x}(t)$. The empirical correlation matrix can be replaced with an exponentially weighted time recursive estimate [12] as

$$\boldsymbol{C}_{xx}(t) = \beta \boldsymbol{C}_{xx}(t-1) + (1-\beta) \overline{\boldsymbol{x}}(t) \overline{\boldsymbol{x}}^T(t)$$

where $\overline{\boldsymbol{x}}(t)$ is the centered measurement vector and β is a forgetting factor. However, as suggested in [14], appropriate measure should be incorporated to account for the change of mean in the aforementioned estimation. The exponentially weighted correlation matrix estimate is then modified to

$$\boldsymbol{C}_{xx}(t) = \beta \left[\boldsymbol{C}_{xx}(t-1) + \Delta \boldsymbol{\mu}(t) \Delta \boldsymbol{\mu}^T(t) \right] + (1-\beta) \overline{\boldsymbol{x}}(t) \overline{\boldsymbol{x}}^T(t) \tag{5}$$

where $\Delta \boldsymbol{\mu}(t) = \boldsymbol{\mu}(t) - \boldsymbol{\mu}(t-1)$ and $\boldsymbol{\mu}(t)$ is the mean estimate of $\boldsymbol{x}(t)$. The major PCs $\boldsymbol{U}_B(t)$ and their corresponding eigenvalues $\boldsymbol{\Lambda}_B(t) = \mathrm{diag}\{\lambda_1(t), \lambda_2(t), \ldots, \lambda_B(t)\}$ at time instant t can be obtained by invoking ED on $\boldsymbol{C}_{xx}(t)$ in (5). This is referred to as the EWM-PCA [12], [13]. On the other hand, in the R-PCA, they are obtained by means of recursively computing $\boldsymbol{C}_{xx}(t)$ as two rank-1 modifications described in [14].

B. Conventional Fault Detection Criteria

For fault detection, the SPE and the T^2 score [28], [29] are two commonly used fault detection measures to visualize the distance of $\boldsymbol{x}(t)$ from the rest of the data. After centering, the SPE for the measurement vector $\overline{\boldsymbol{x}}(t)$ is given by

$$\mathrm{SPE}(t) = \|\overline{\boldsymbol{x}}(t) - \hat{\boldsymbol{x}}(t)\|_2^2 \tag{6}$$

where $\hat{\boldsymbol{x}}(t)$ is the approximated measurement and it can be determined according to (4) as

$$\hat{\boldsymbol{x}}(t) = \boldsymbol{U}_B(t) \boldsymbol{U}_B^T(t) \overline{\boldsymbol{x}}(t). \tag{7}$$

Note that only the major subspace $\boldsymbol{U}_B(t)$ is required in computing the SPE. The measurement vector is labeled as a faulty sample when the SPE exceeds a certain detection threshold. Conventionally, the detection threshold for the SPE is given by [28] and [29]

$$\Gamma_{\mathrm{SPE}}(t) = \theta_1(t) \left[\frac{h_0 \xi \sqrt{2\theta_2(t)}}{\theta_1(t)} + 1 + \frac{\theta_2(t) h_0(t) (h_0(t) - 1)}{\theta_1^2(t)} \right]^{\frac{1}{h_0(t)}} \tag{8}$$

where $h_0(t) = 1 - (2\theta_1(t)\theta_3(t)/3\theta_1^2(t))$, $\theta_j(t) = \Sigma_{b=B+1}^{P} \lambda_b^j(t)$, $j = 1, 2, 3$, $\lambda_b(t)$ is the bth largest eigenvalue of $\boldsymbol{C}_{xx}(t)$ in (5), and ξ is a threshold quartile parameter corresponding to the upper $(1 - P\{X > \xi\})$ percentile of the Gaussian distribution. Hence, the probability that the faulty sample exceeds the threshold quartile is $P\{X > \xi\} = (2/\sqrt{\pi}) \int_{\xi}^{\infty} e^{-x^2} dx$. The value of ξ is chosen to achieve a certain detection rate. In process

monitoring, the mean process is usually slow varying, and a detection confidence interval of $P\{-\xi \leq X < \xi\} = 0.99$ is often used [12], [30]. The detection threshold in (8) depends on the quadratic and cubic sum of the eigenvalues, and therefore, it could be sensitive to the effect of the faulty samples on the eigenvalues.

On the other hand, the T^2 score for the measurement vector $\overline{\boldsymbol{x}}(t)$ is given by

$$T^2(t) = \left\|\overline{\boldsymbol{x}}^T(t)\boldsymbol{U}_B(t)\boldsymbol{\Lambda}_B^{-1}(t)\boldsymbol{U}_B^T(t)\overline{\boldsymbol{x}}(t)\right\|_2^2 \tag{9}$$

where $\boldsymbol{\Lambda}_B(t)$ contains the first B largest eigenvalues obtained from $\boldsymbol{C}_{xx}(t)$ in (5). Note that, in computing the T^2 score, the eigenvalues at each time instant are required. The T^2 score is based on the first B PCs, and it detects the changes in the latent variables that are of the greatest importance to the variance of the process. The detection threshold for the T^2 score is given by

$$\Gamma_{T^2}(t) = \frac{(P^2-1)B}{P(P-B)}\xi_F \tag{10}$$

where ξ_F is a threshold quartile parameter of the F distribution with B and $P-B$ degrees of freedom. For the same confidence interval $P\{-\xi \leq X < \xi\}$, the value of ξ_F is related to ξ as follows:

$$\xi_F = F^{-1}\left(P\{-\xi \leq X < \xi\}\right) \tag{11}$$

where $F^{-1}(.)$ is the inverse cumulative distribution function of the F distribution. Note that the detection threshold in (10) is independent of time, and hence, it may be less adaptive to gradual system change. Faulty samples can be labeled using one of the following criteria:

1) SPE-based detection criterion: The SPE exceeds the detection threshold.
2) T^2 score-based detection criterion: The T^2 score exceeds the detection threshold.
3) SPE + T^2 score-based detection criterion: Either the T^2 score or the SPE exceeds their detection thresholds.

Among the three criteria, the SPE + T^2 score-based detection criterion is most commonly adopted because both measures are complement to each other for the fault detection in either signal or noise subspaces [31]. In other words, the use of both measures allows one to identify faults in both the signal and noise subspaces, thus increasing the accuracy of fault detection.

When a faulty sample is detected, its masking effect on subsequent faults should be isolated by either removing the faulty sample or by estimating its effect in detecting subsequent faulty samples, which is commonly referred to as fault replacement [8]. In this paper, we consider the former option (i.e., the removal of the faulty sample) for simplicity and develop an efficient fault detection approach based on the subspace principle. In principle, the effect of the detected faults can also be estimated from the estimated PCs. For more details of fault replacement, interested readers are referred to [8].

III. Proposed Subspace-Tracking-Based Fault Detection Algorithms

In this paper, we mainly focus on the local detection used in the distributed approach for simplicity. Interested readers are referred to [9] for a comprehensive study of the PCA in a distributed architecture. In the PCA approach, outlier detection is performed by analyzing the collected raw measurements with a normal operation model, which consists of the mean estimate, the PCs that span the signal subspace, and a detection threshold. The normal operation model is usually built offline using a fixed block of initial data. Its major disadvantage is that it does not take into account gradual system changes because the model and detection threshold are fixed. On the other hand, in the proposed approach, the normal operation model and detection threshold are updated recursively so that it is more adaptive to gradual system changes.

The proposed approach can be mainly divided into three steps:

1) A new robust recursive location estimator is proposed to update the mean estimate recursively.
2) Then, the proposed robust subspace tracking algorithms are used to estimate the signal subspace recursively.
3) New robust detection criteria are proposed to perform fault detection and compute the detection thresholds required in the robust subspace tracking algorithms. The robust subspace tracking algorithms ignore the sample when an outlier sample is detected and perform normal update otherwise.

In the next section, we shall describe the recursive implementation of the fault detection algorithms.

A. Robust Recursive Location Estimator

A conventional recursive mean estimator of $\boldsymbol{x}(t)$ is

$$\boldsymbol{\mu}(t) = \boldsymbol{\mu}(t-1) + \frac{1}{t}\left(\boldsymbol{x}(t) - \boldsymbol{\mu}(t-1)\right) \tag{12}$$

where $\boldsymbol{\mu}(t)$ is the recursive sample mean obtained at time instant t and $\boldsymbol{x}(t)$ is the raw measurement vector obtained at time instant t. For online implementation, the data in the distant past should be given less weighting to reflect changes in the process. Therefore, a forgetting factor β with a value less than but close to one is usually introduced to form the following recursive estimator:

$$\boldsymbol{\mu}(t) = \beta\boldsymbol{\mu}(t-1) + (1-\beta)\boldsymbol{x}(t). \tag{13}$$

However, this estimator is sensitive to impulsive noise since a single impulse with large amplitude in $\boldsymbol{x}(t)$ can substantially increase the values of $\boldsymbol{\mu}(t)$. Therefore, the influence of faulty samples on the estimation of the PCs can be unbounded. In the statistical communities, a commonly used robust location estimator is the median. For online implementation, we propose the following recursive robust location estimate:

$$\boldsymbol{\mu}(t) = \beta\boldsymbol{\mu}(t-1) + (1-\beta)\mathrm{med}\left(A\left(\boldsymbol{x}(t)\right)\right) \tag{14}$$

where $A(\boldsymbol{x}(t)) = \{\boldsymbol{x}(t)\}, \ldots, \boldsymbol{x}(t-L+1)\}$, $\mathrm{med}(.)$ is the median operator, and the window length is L. To reduce the

TABLE I
OPAST ALGORITHM

Initialization:

- Initialize $\boldsymbol{\mu}(0) = \text{mean}(\boldsymbol{X}(0))$, where $\boldsymbol{X}(0)$ is an initial data block.
- Kaiser's rule is applied to $\boldsymbol{X}(0)$ to estimate the signal subspace dimension B.
- Obtain $\boldsymbol{U}_B(0)$ and $\boldsymbol{\Lambda}_B(0)$ from the ED of $\boldsymbol{C}_{xx}(0) = (1/N_0)\boldsymbol{X}^T(0)\boldsymbol{X}(0)$, where N_0 is the number of measurements in the initial data block.
- $\boldsymbol{W}(0) = \boldsymbol{U}_B(0)$, $\boldsymbol{C}_{yy}(0) = \boldsymbol{W}^T(0)\boldsymbol{C}_{xx}(0)\boldsymbol{W}(0)$, $\boldsymbol{\Omega}(0) = \boldsymbol{C}_{yy}^{-1}(0)$.
- β is the forgetting factor. (Typical value 0.99)

Recursion:

For $t = 1,2\cdots, T$ *do*

$$\boldsymbol{y}(t) = \boldsymbol{W}^T(t-1)\overline{\boldsymbol{x}}(t),$$

$$\boldsymbol{g}(t) = \frac{1}{\beta}\boldsymbol{\Omega}(t-1)\boldsymbol{y}(t),$$

$$\gamma(t) = \frac{1}{1+\boldsymbol{y}^H(t)\boldsymbol{g}(t)},$$

$$\boldsymbol{p}(t) = \gamma(t)\big(\overline{\boldsymbol{x}}(t) - \boldsymbol{W}(t-1)\boldsymbol{y}(t)\big),$$

Orthonormalization Step for the estimated subspace

$$\tau(t) = \frac{1}{\|\boldsymbol{g}(t)\|_2^2}\left(\frac{1}{\sqrt{1+\|\boldsymbol{p}(t)\|_2^2\|\boldsymbol{g}(t)\|_2^2}} - 1\right),$$

$$\boldsymbol{p}'(t) = \tau(t)\boldsymbol{W}(t-1)\boldsymbol{g}(t) + (1+\tau(t)\|\boldsymbol{g}(t)\|_2^2)\boldsymbol{p}(t),$$

Update:

$$\boldsymbol{W}(t) = \boldsymbol{W}(t-1) + \boldsymbol{p}'(t)\boldsymbol{g}^T(t),$$

$$\boldsymbol{\Omega}(t) = \frac{1}{\beta}\boldsymbol{\Omega}(t-1) - \gamma(t)\boldsymbol{g}(t)\boldsymbol{g}^T(t).$$

End for

operations required for the median filter in practical implementation, the length of estimation window is usually chosen from 5 to 11 [32]. For large L, the pseudomedian [33] can be used to reduce the computational complexity. The centered measurement vector using the recursive mean estimate in (14), i.e.,

$$\overline{\boldsymbol{x}}(t) = \boldsymbol{x}(t) - \boldsymbol{\mu}(t) \tag{15}$$

is then used in the recursive estimation of the signal subspace.

B. Proposed Subspace Tracking Approach

As mentioned earlier, the arithmetic complexity of conventional PCA-based fault detection algorithms is costly for online applications because they require the computation of the entire ED. To reduce the arithmetic complexity for fault detection, we shall propose new algorithms based on the subspace tracking concept [15]–[18]. Particularly, the signal subspace spanned by the major PCs $\boldsymbol{U}_B(t)$ is tracked recursively instead of computing the entire ED. A classical algorithm is the PAST algorithm proposed in [17]. The PAST algorithm recursively estimates the signal subspace by minimizing the following objective function:

$$J(\boldsymbol{W}(t)) = \sum_{i=1}^{t} \beta^{t-i}\,\|\overline{\boldsymbol{x}}(i) - \boldsymbol{W}(t)\boldsymbol{y}(i)\|_2^2. \tag{16}$$

Ideally, $\boldsymbol{y}(i) = \boldsymbol{W}^T(t)\overline{\boldsymbol{x}}(i)$, and $J(\boldsymbol{W}(t))$ represents the energy in $\overline{\boldsymbol{x}}(i)$ which is outside the subspace $\boldsymbol{W}(t)$. Hence, $\boldsymbol{W}(t)$ is equal to the major PCs $\boldsymbol{U}_B(t)$ up to an orthogonal transformation or rotation, i.e., $span(\boldsymbol{W}(t)) = span(\boldsymbol{U}_B(t))$. Hence, the outer product $\boldsymbol{W}(t)\boldsymbol{W}^T(t)$ is equal to $\boldsymbol{U}_B(t)\boldsymbol{U}_B^T(t)$. In the PAST algorithm, the projection approximation $\overline{\boldsymbol{y}}(i) \approx \boldsymbol{W}^T(i-1)\overline{\boldsymbol{x}}(i)$ is employed so that (16) can be relaxed to a quadratic function in $\boldsymbol{W}(t)$. Consequently, conventional recursive least squares algorithm can be applied to solve for $\boldsymbol{W}(t)$ with very low arithmetic complexity. In the OPAST algorithm [18], an extra orthonormalization step is added to the PAST algorithm to guarantee the orthonormality of the estimated subspace $\boldsymbol{W}(t)$.

To apply the OPAST algorithm for fault detection, an initial ED is assumed to be available either by performing an ED on an initial data block or predetermining the eigenvalues offline. The eigenvalues so obtained are used with the Kaiser's rule [34] or the minimum description length (MDL) [35] to estimate the dimension B of the signal subspace. During online application, the OPAST algorithm is invoked to update the signal subspace recursively. Table I summarizes the OPAST algorithm.

It should be noted that, since the outer product $\boldsymbol{W}(t)\boldsymbol{W}^T(t)$ is equal to $\boldsymbol{U}_B(t)\boldsymbol{U}_B^T(t)$, the *SPE* can be computed as

$$SPE(t) = \left\|\overline{\boldsymbol{x}}(t) - \boldsymbol{W}(t)\boldsymbol{W}^T(t)\overline{\boldsymbol{x}}(t)\right\|_2^2 \tag{17}$$

which does not require the eigenvalues and eigenvectors. If only the SPE is needed for outlier detection, the OPAST algorithm can be used and the arithmetic complexity will be much lower than conventional PCA-based algorithms. On the other hand, as the computation of T^2 score requires both the eigenvalues

$\boldsymbol{\Lambda}_B(t)$ and eigenvectors $\boldsymbol{U}_B(t)$, the OPAST algorithm is not directly applicable. To overcome this problem, one may employ the R-PCA in [14] to recursively compute the ED of $\boldsymbol{C}_{xx}(t)$ in (5) as two rank-1 modifications.

To further reduce the complexity, we propose, in this paper, to compute the required subspace using subspace tracking algorithms such as the OPAST algorithm. By projecting the signal vector on this subspace, one can compute recursively the ED of the projected covariance matrix and hence the required eigenvectors and eigenvalues in the desired subspace. This results in lower arithmetic complexity, when comparing with the R-PCA algorithm, because the dimension of the projected correlation matrix is smaller than that of the original correlation matrix in (5). For the sake of presentation, it is called the OPASTr algorithm.

An alternative with even lower arithmetic complexity is to compute the eigenvalues and eigenvectors in the desired subspace using the PAST algorithm with deflation (PASTd) in [17]. Similarly, an extra orthonormalization step can be added to the PASTd algorithm at each iteration, and it is referred to as the OPASTd algorithm in this paper.

Due to page limitation, the detailed derivations of the PAST, the PASTd, and the OPAST algorithms are omitted, and interested readers are referred to [17] and [18] for more details. The details for computing the eigenvalues and eigenvectors in the OPASTr and OPASTd algorithms will now be given.

C. Recursive Eigenvalue and Eigenvector Computation

In the PAST algorithm, it is known that the estimated subspace $\boldsymbol{W}(t)$ is equal to the major PCs $\boldsymbol{U}_B(t)$ up to an orthogonal transformation or rotation $\boldsymbol{Q}(t)$, i.e.,

$$\boldsymbol{U}_B(t) = \boldsymbol{W}(t)\boldsymbol{Q}(t) \tag{18}$$

where $\boldsymbol{Q}(t)$ is a $B \times B$ orthogonal matrix satisfying $\boldsymbol{Q}(t)\boldsymbol{Q}^T(t) = \boldsymbol{I}$. We now propose an approach based on rank-1 modification to estimate the associated eigenvectors and eigenvalues of the subspace and employ them for fault detection. More precisely, one can project the centered measurement vector $\overline{\boldsymbol{x}}(t)$ on $\boldsymbol{W}(t)$ to get $\boldsymbol{y}(t) = \boldsymbol{W}^T(t)\overline{\boldsymbol{x}}(t)$. Here, we remark that $\boldsymbol{y}(t)$ is a projection of $\overline{\boldsymbol{x}}(t)$ on the subspace $\boldsymbol{W}(t)$, and it is different from the projection approximation $\overline{\boldsymbol{y}}(t)$ in (16). Let the resultant correlation matrix of $\boldsymbol{y}(t)$ be $\boldsymbol{C}_{yy}(t) = E[\boldsymbol{y}(t)\boldsymbol{y}^T(t)]$. If $\boldsymbol{W}(t)$ is slowly varying over time, then $\boldsymbol{C}_{yy}(t) = \boldsymbol{W}^T(t)\boldsymbol{C}_{xx}(t)\boldsymbol{W}(t)$. By projecting $\boldsymbol{C}_{xx}(t)$ onto the signal subspace $\boldsymbol{W}(t)$, and from (18), we obtain

$$\begin{aligned}\boldsymbol{C}_{yy}(t) &= \boldsymbol{W}^T(t)\boldsymbol{U}(t)\boldsymbol{\Lambda}(t)\boldsymbol{U}^T(t)\boldsymbol{W}(t)\\ &= \boldsymbol{W}^T(t)\boldsymbol{U}_B(t)\boldsymbol{\Lambda}_B(t)\boldsymbol{U}_B^T(t)\boldsymbol{W}(t)\\ &= \boldsymbol{Q}(t)\boldsymbol{\Lambda}_B(t)\boldsymbol{Q}^T(t).\end{aligned} \tag{19}$$

By means of the projection, only the eigenvectors that span the signal subspace are retained. Hence, the eigenvectors of the transformation $\boldsymbol{Q}(t)$ can be computed using the ED or SVD of $\boldsymbol{C}_{yy}(t)$. As mentioned earlier, the complexity of both methods is very costly for real-time applications. Fortunately, it is known that [36] the ED of the rank-1 update can be recursively computed. More precisely, given the ED of a matrix $\boldsymbol{C} = \boldsymbol{U}\boldsymbol{\Lambda}\boldsymbol{U}^T$, we are interested in computing the ED of the rank-1 update of $\boldsymbol{C}$: $\widetilde{\boldsymbol{C}} = \boldsymbol{C} + \rho'\boldsymbol{x}\boldsymbol{x}^T$, which can be rewritten as $\widetilde{\boldsymbol{C}} = \boldsymbol{U}(\Lambda + \rho\boldsymbol{z}\boldsymbol{z}^T)\boldsymbol{U}^T$ with $\boldsymbol{z} = \boldsymbol{U}^T\boldsymbol{x}/\|\boldsymbol{U}^T\boldsymbol{x}\|_2$ and $\rho = \rho'\|\boldsymbol{U}^T\boldsymbol{x}\|_2^2$. In other words, the problem is reduced to computing the ED of the rank-1 update of $\widetilde{\boldsymbol{\Lambda}}$: $(\boldsymbol{\Lambda}_0 + \rho\boldsymbol{z}\boldsymbol{z}^T)$, where ρ is a scalar and $\boldsymbol{z}$ is a vector of unit norm. It has been shown that [36] the eigenvalues $\overline{\lambda}_j$ can be updated by finding the roots of the following secular equation:

$$f(\lambda) = 1 + \rho\sum_{j=1}^{P}\frac{z_j^2}{(\lambda_j - \lambda)} \tag{20}$$

where z_j is the jth element of z and λ_j is the jth diagonal value of $\boldsymbol{\Lambda}_0$. After solving the secular equation, the jth eigenvector can be updated as follows:

$$\widetilde{\boldsymbol{u}}_j = \frac{(\boldsymbol{\Lambda}_0 - \widetilde{\lambda}_j\boldsymbol{I})^{-1}\boldsymbol{z}}{\left\|(\boldsymbol{\Lambda}_0 - \widetilde{\lambda}_j\boldsymbol{I})^{-1}\boldsymbol{z}\right\|_2} \tag{21}$$

where $\widetilde{\boldsymbol{\Lambda}} = \mathrm{diag}(\widetilde{\lambda}_1, \ldots, \widetilde{\lambda}_P)$ contains the estimated eigenvalues obtained from the secular equation in (20). Hence, the ED of $\widetilde{\boldsymbol{C}}$ can be updated as $\widetilde{\boldsymbol{U}}\widetilde{\boldsymbol{\Lambda}}\widetilde{\boldsymbol{U}}^T$, where $\widetilde{\boldsymbol{U}} = [\widetilde{\boldsymbol{u}}_1, \ldots, \widetilde{\boldsymbol{u}}_P]$. We now extend this technique to our recursive eigenvector and eigenvalue computation of the subspace components in the OPASTr algorithm.

Similar to (5), the correlation matrix $\boldsymbol{C}_{yy}(t) = E[\boldsymbol{y}(t)\boldsymbol{y}^T(t))]$ in (19) can be recursively updated as

$$\boldsymbol{C}_{yy}(t) = \beta\boldsymbol{C}_{yy}(t-1) + (1-\beta)\boldsymbol{y}(t)\boldsymbol{y}^T(t). \tag{22}$$

Unlike (5), the change of mean is not incorporated in (22) because the projection $\boldsymbol{y}(t) = \boldsymbol{W}(t)\overline{\boldsymbol{x}}(t)$ is obtained from the centered measurement vector $\overline{\boldsymbol{x}}(t)$, and hence, centering is not required for $\boldsymbol{y}(t)$. First, let the ED of $\boldsymbol{C}_{yy}(t-1)$ be $\boldsymbol{Q}(t-1)\boldsymbol{\Lambda}_B(t-1)\boldsymbol{Q}^T(t-1)$. The expression in (22) can be rewritten as one rank-1 modification given by

$$\boldsymbol{C}_{yy}(t) = \boldsymbol{Q}(t-1)\left[\beta\boldsymbol{\Lambda}_B(t-1) + (1-\beta)\boldsymbol{z}(t)\boldsymbol{z}^T(t)\right]\boldsymbol{Q}(t-1)^T \tag{23}$$

where $\boldsymbol{z}(t) = \boldsymbol{Q}^T(t-1)\boldsymbol{y}(t)$. Let the corresponding ED be

$$\beta\boldsymbol{\Lambda}_B(t-1) + (1-\beta)\boldsymbol{z}(t)\boldsymbol{z}^T(t) = \widetilde{\boldsymbol{Q}}(t)\boldsymbol{\Lambda}_B(t)\widetilde{\boldsymbol{Q}}^T(t). \tag{24}$$

Consequently, the new eigenvalues and eigenvectors can be computed according to (20) and (21). The term inside the square bracket in (23) is recognized as a rank-1 modification mentioned earlier with $\boldsymbol{\Lambda}_0 = \beta\boldsymbol{\Lambda}_B(t-1)$, $\rho = (1-\beta)\|\boldsymbol{z}_\mu(t)\|_2^2$, and $\boldsymbol{z} = \boldsymbol{z}(t)/\|\boldsymbol{z}(t)\|_2$. Finally, the eigenvectors of $\boldsymbol{C}_{yy}(t)$ are given by

$$\boldsymbol{Q}(t) = \boldsymbol{Q}(t-1)\widetilde{\boldsymbol{Q}}(t). \tag{25}$$

Using this result, the PCs $\boldsymbol{U}_B(t)$ can be obtained from (18). The secular equation in (20) is usually solved by some Newton-like algorithms, and the average number of iterations for convergence is 4.4 [36]. The complexity of the rank-1 modification is $O(B^3)$ floating point operations (flops) per iteration. Interested readers are referred to [37] for a comprehensive study of the rank-1 modifications.

Unlike the OPASTr algorithm, the OPASTd uses a deflation approach, which is motivated by the PASTd algorithm

in [17], to sequentially compute the eigenvectors and eigenvalues of the projection correlation matrix $\boldsymbol{C}_{yy}(t)$ in (19). More specifically, we denote the bth eigenvalue of $\boldsymbol{C}_{yy}(t)$ as $\lambda_b(t)$ and the bth eigenvector as $\boldsymbol{q}_b(t)$ such that $\boldsymbol{Q}(t) = [\boldsymbol{q}_1(t), \boldsymbol{q}_2(t), \ldots, \boldsymbol{q}_B(t)]$. At the bth iteration, $\lambda_b(t)$ and $\boldsymbol{q}_b(t)$ are first updated as

$$\lambda_b(t) = \beta\lambda_b(t-1) + |z_b(t)|_2^2 \tag{26}$$

$$\boldsymbol{q}_b(t) = \boldsymbol{q}_b(t-1) + \boldsymbol{e}_b(t)\left[z_b^*(t)/\lambda_b(t)\right] \tag{27}$$

respectively, where

$$z_b(t) = \boldsymbol{q}_b^T(t-1)\boldsymbol{r}^{(b)}(t) \tag{28}$$

$$\boldsymbol{e}_b(t) = \boldsymbol{r}^{(b)}(t) - \boldsymbol{q}_b(t-1)z_b(t) \tag{29}$$

the superscript $*$ denotes the complex conjugate, β is the forgetting factor introduced in (5), and $\boldsymbol{r}^{(b)}(t)$ ($\boldsymbol{r}^{(1)}(t) = \boldsymbol{y}(t)$) denotes the residue vector obtained by removing the first $(b-1)$ projections from $\boldsymbol{y}(t)$. Then, the projection of $\boldsymbol{r}^{(b)}(t)$ onto $\boldsymbol{q}_b(t)$ is removed from $\boldsymbol{r}^{(b)}(t)$ using the following formula:

$$\boldsymbol{r}^{(b+1)}(t) = \boldsymbol{r}^{(b)}(t) - \boldsymbol{q}_b(t)z_b(t). \tag{30}$$

The aforementioned deflation approach can be repeated B times for the computation of all B major eigenvectors and their associated eigenvalues. After obtaining $\boldsymbol{Q}(t)$, the major PCs $\boldsymbol{U}_B(t)$ can be obtained similarly from (18). It can be seen that the sequential nature of the PASTd algorithm significantly reduces the arithmetic complexity. However, the orthonormality of the subspace may not be guaranteed, and hence, it is less accurate. This will be illustrated by the simulation results in Section IV-D.

D. Robust Recursive Detection Criteria

The detection of possible faulty samples using SPE and T^2 score relies critically on the selection of appropriate threshold. Furthermore, to make the detection adaptive to gradual changes in system parameters, this threshold should be recursively updated from the measurements. In this paper, we propose to employ the robust SPE and robust T^2 score for fault detection, which are derived from the robust $\boldsymbol{z}$-score reported in [24] for outlier detection.

An important advantage of using these robust statistics [23] is that they are more robust to the adverse influence of faulty samples. To facilitate online implementation, we shall propose a recursive implementation of the robust SPE and robust T^2 score. More precisely, a fault or outlier is said to be occurred when

$$|SPE(t) - \mu_{\mathrm{SPE}}(t)| \geq \xi\sigma_{\mathrm{SPE}}(t) \tag{31}$$

$$\left|T^2(t) - \mu_{T^2}(t)\right| \geq \xi\sigma_{T^2}(t) \tag{32}$$

where $\mu_{\mathrm{SPE}}(t)$ and $\mu_{T^2}(t)$ are robust location estimates of $SPE(t)$ in (17) and $T^2(t)$ in (9), respectively, and $\sigma_{\mathrm{SPE}}(t)$ and $\sigma_{T^2}(t)$ are robust scale estimators of $SPE(t)$ and $T^2(t)$, respectively. We can see that the computation of robust SPE and robust T^2 score in (31) and (32) only requires the eigenvectors and eigenvalues of the tracked subspace, which is in contrast to their conventional counterparts in (8) and (10), respectively. Motivated by [32] and [38], the following robust recursive location and variance estimates for the robust SPE and robust T^2 score are proposed:

$$\begin{aligned}\mu_{\mathrm{SPE}}(t) = {} & \beta_{\mu\_\mathrm{SPE}}\mu_{\mathrm{SPE}}(t-1) \\ & + (1-\beta_{\mu\_\mathrm{SPE}})\mathrm{med}\left(A\left(SPE(t)\right)\right)\end{aligned} \tag{33}$$

$$\begin{aligned}\sigma_{\mathrm{SPE}}^2(t) = {} & \beta_{\sigma\_\mathrm{SPE}}\sigma_{\mathrm{SPE}}^2(t-1) \\ & + c(1-\beta_{\sigma\_\mathrm{SPE}})\mathrm{med}\left(A\left(\Delta_{\mathrm{SPE}}(t)^2\right)\right)\end{aligned} \tag{34}$$

$$\begin{aligned}\mu_{T^2}(t) = {} & \beta_{\mu\_T^2}\mu_{T^2}(t-1) \\ & + (1-\beta_{\mu\_T^2})\mathrm{med}\left(A\left(T^2(t)\right)\right)\end{aligned} \tag{35}$$

$$\begin{aligned}\sigma_{T^2}^2(t) = {} & \beta_{\sigma\_T^2}\sigma_{T^2}^2(t-1) \\ & + c(1-\beta_{\sigma\_T^2})\mathrm{med}\left(A\left(\Delta_{T^2}(t)^2\right)\right)\end{aligned} \tag{36}$$

where β_{μ_SPE}, $\beta_{\sigma\_\mathrm{SPE}}$, $\beta_{\mu\_T^2}$, and $\beta_{\sigma\_T^2}$ are positive forgetting factors close to but less than one; $A(d(t)) = \{d(t), d(t-1), \ldots, d(t-L_d+1)\}$ with L_d being the window length and $d(t)$ denoting either $SPE(t)$, $T^2(t)$, $\Delta_{\mathrm{SPE}}(t)$, or $\Delta_{T^2}(t)$; $\mathrm{med}(.)$ is the median operator; $c = 2.13$ is a correction factor for Gaussian input; and $\Delta_{\mathrm{SPE}}(t)$ and $\Delta_{T^2}(t)$ are instantaneous deviations of the $SPE(t)$ and $T^2(t)$ scores, respectively, from their robust estimates

$$\Delta_{\mathrm{SPE}}(t) = SPE(t) - \mu_{\mathrm{SPE}}(t) \tag{37}$$

$$\Delta_{T^2}(t) = T^2(t) - \mu_{T^2}(t). \tag{38}$$

The use of the median operator is to remove possible outliers in $SPE(t)$ and $T^2(t)$ from affecting the recursive mean (location) and variance (dispersion) estimates. Next, we will discuss how the subspace tracking algorithms should be modified when an outlier is encountered.

E. Robust Subspace Tracking

Although the subspace-based algorithms introduced earlier significantly reduce the arithmetic complexity, they are sensitive to impulsive outliers [23]. This is because the large amplitudes of the faulty samples will significantly affect the tracking of the subspaces and the updating of the threshold for further fault detection. Next, we extend the OPASTr and OPASTd algorithms to improve their robustness to impulsive faults. The resulting algorithms are called the R-OPASTr and R-OPASTd algorithms, respectively.

The proposed robust OPASTr and OPASTd algorithms are extensions of the robust PAST algorithm in [32], which relies on a robust recursive covariance estimate based on M-estimation [22]. More specifically, the proposed robust recursive covariance estimate is modified from the covariance estimate in (5) as

$$\begin{aligned}\boldsymbol{C}_{\rho\_xx}(t) = {} & \psi\left(\overline{\boldsymbol{x}}(t)\right)\beta\left[\boldsymbol{C}_{\rho\_xx}(t-1) + \Delta\boldsymbol{\mu}(t)\Delta\boldsymbol{\mu}^T(t)\right] \\ & + \psi\left(\overline{\boldsymbol{x}}(t)\right)(1-\beta)\overline{\boldsymbol{x}}(t)\overline{\boldsymbol{x}}^T(t) + \left(1-\psi\left(\overline{\boldsymbol{x}}(t)\right)\right)\boldsymbol{C}_{\rho\_xx}(t-1)\end{aligned} \tag{39}$$

where $\psi(\overline{\boldsymbol{x}}(t))$ is a robust weight function. Ideally, if $\overline{\boldsymbol{x}}(t)$ is an outlier, $\psi(\overline{\boldsymbol{x}}(t))$ should be small so that the covariance matrix $\boldsymbol{C}_{\rho\_xx}(t)$ will not be affected by the corrupted samples. Otherwise, it should be equal to one as in normal updating. In [32], $\psi(\overline{\boldsymbol{x}}(t))$ is chosen as $q_H(\|\overline{\boldsymbol{x}}(t)\|_2)$, where $q_H(u) = \begin{cases} 1 & u_H \\ 0 & \text{otherwise} \end{cases}$ is the derivative of the modified Huber M-estimate function and Γ_H is a threshold for suppressing the

TABLE II
PROPOSED R-OPASTr ALGORITHM

Initialization:

Initialize $\boldsymbol{\mu}(0), \boldsymbol{U}_B(0), \boldsymbol{\Lambda}_B(0), \boldsymbol{W}(0), \boldsymbol{C}_{yy}(0), \boldsymbol{\Omega}(0)$ and β as in Table I.

Initialize $\boldsymbol{Q}(0)$ as the eigenvectors of the ED of $\boldsymbol{C}_{yy}(0)$.

Recursion:

For $t = 1,2\cdots, T$ *do*

$\boldsymbol{\mu}(t) = \beta\boldsymbol{\mu}(t-1) + (1-\beta)\text{med}(A(\boldsymbol{x}(t)))$,

$\overline{\boldsymbol{x}}(t) = \boldsymbol{x}(t) - \boldsymbol{\mu}(t)$.

Update $\boldsymbol{W}(t)$ and $\boldsymbol{\Omega}(t)$ with the OPAST algorithm in Table I.

Case:

Robust SPE:
- Compute $\text{SPE}(t)$ using (17).
- Update $\mu_{\text{SPE}}(t)$, $\sigma_{\text{SPE}}(t)$ as in (33), (34).

Robust T^2 score:
- Update $\boldsymbol{Q}(t)$ and $\boldsymbol{\Lambda}_B(t)$ by the proposed new recursive method based on rank-1 modification in (19) - (25).
- Compute $\boldsymbol{U}_B(t) = \boldsymbol{W}(t)\boldsymbol{Q}(t)$ using (18).
- Compute $T^2(t)$ using (9).
- Update $\mu_{T^2}(t)$, $\sigma_{T^2}(t)$ using (35), (36).

Robust SPE + T^2 score :
- Compute both Robust SPE and Robust T^2 score as above.

End Case

Robust subspace update

Update $\psi(\overline{\boldsymbol{x}}(t))$ using (40) - (43)

If $\psi(\overline{\boldsymbol{x}}(t)) = 0$ (outlier is detected)

$\boldsymbol{W}(t) = \boldsymbol{W}(t-1)$,

$\boldsymbol{\Omega}(t) = \boldsymbol{\Omega}(t-1)$,

$\boldsymbol{\Lambda}_B(t) = \boldsymbol{\Lambda}_B(t-1)$,

$\boldsymbol{U}_B(t) = \boldsymbol{U}_B(t-1)$.

End if

End for

TABLE III
PROPOSED R-OPASTd ALGORITHM

Initialization:

Initialize $\boldsymbol{\mu}(0), \boldsymbol{U}_B(0), \boldsymbol{\Lambda}_B(0), \boldsymbol{W}(0), \boldsymbol{C}_{yy}(0), \boldsymbol{\Omega}(0), \boldsymbol{Q}(0)$ and β as in Table II.

Recursion:

For $t = 1,2\cdots, T$ *do*

$\boldsymbol{\mu}(t) = \beta\boldsymbol{\mu}(t-1) + (1-\beta)\text{med}(A(\boldsymbol{x}(t)))$,

$\overline{\boldsymbol{x}}(t) = \boldsymbol{x}(t) - \boldsymbol{\mu}(t)$,

Update $\boldsymbol{W}(t)$ and $\boldsymbol{\Omega}(t)$ with the OPAST algorithm in Table I.

Case:

Robust SPE:
- Compute $\text{SPE}(t)$ using (17).
- Update $\mu_{\text{SPE}}(t)$, $\sigma_{\text{SPE}}(t)$ as in (33), (34).

Robust T^2 score:
- Update $\boldsymbol{Q}(t)$ and $\boldsymbol{\Lambda}_B(t)$ by the proposed deflation approach in (26) - (30).
- Compute $\boldsymbol{U}_B(t) = \boldsymbol{W}(t)\boldsymbol{Q}(t)$.
- Compute $T^2(t)$ using (9).
- Update $\mu_{T^2}(t)$, $\sigma_{T^2}(t)$ using (35), (36).

Robust SPE+ T^2 score :
- Compute both Robust SPE and Robust T^2 score as above.

End Case

Robust subspace update

Update $\psi(\overline{\boldsymbol{x}}(t))$ using (40) - (43)

If $\psi(\overline{\boldsymbol{x}}(t)) = 0$ (outlier is detected)

$\boldsymbol{W}(t) = \boldsymbol{W}(t-1)$,

$\boldsymbol{\Omega}(t) = \boldsymbol{\Omega}(t-1)$,

$\boldsymbol{\Lambda}_B(t) = \boldsymbol{\Lambda}_B(t-1)$,

$\boldsymbol{U}_B(t) = \boldsymbol{U}_B(t-1)$.

End if

End for

adverse effect of faulty samples. In other words, the modified Huber function simply ignores the samples when an outlier is detected and proceeds with normal updating otherwise. Note that other more complicated M-estimate function such as the Hampel's function [23] can be used to suppress the contribution of the samples to different extents. For simplicity, we shall employ the modified Huber function in this paper.

Since the T^2 score and SPE will be employed for outlier detection, it is more convenient to choose $\psi(\overline{\boldsymbol{x}}(t))$ as

$$q_{T^2}(\Delta_{T^2}(t)) = \begin{cases} 1, & |\Delta_{T^2}(t)| < \Gamma_{T^2} \\ 0, & \text{otherwise} \end{cases} \tag{40}$$

$$q_{\text{SPE}}(\Delta_{\text{SPE}}(t)) = \begin{cases} 1 & |\Delta_{\text{SPE}}(t)| < \Gamma_{\text{SPE}} \\ 0 & \text{otherwise} \end{cases} \tag{41}$$

or $q_{T^2}(\Delta_{T^2}(t)) \cdot q_{\text{SPE}}(\Delta_{\text{SPE}}(t))$, depending on which criterion is used. Here, $\Delta_{\text{SPE}}(t)$ and $\Delta_{T^2}(t)$ are instantaneous deviations of the $SPE(t)$ and $T^2(t)$ scores from their robust estimates defined in (37) and (38). Γ_{SPE} and Γ_{T^2} are the threshold parameters chosen to control the degree of suppression of the faulty samples.

Motivated by [22], [32], and [38], we further propose to update the thresholds Γ_{SPE} and Γ_{T^2} using the adaptive threshold selection (ATS) method, which are given by

$$\Gamma_{\text{SPE}} = \xi\sigma_{\text{SPE}}(t) \tag{42}$$

$$\Gamma_{T^2} = \xi\sigma_{T^2}(t) \tag{43}$$

where ξ is the threshold quartile parameter introduced in (8). Consequently, the detection thresholds Γ_{SPE} and Γ_{T^2} can be updated recursively, and they are more adaptive to gradual system change.

With the robust covariance update in (39), the conventional PAST objective function in (16) will be modified to the following robust PAST objective function:

$$J(\boldsymbol{W}(t)) = \sum_{i=1}^{t} \beta^{t-i}\psi(\overline{\boldsymbol{x}}(i)) \cdot \|\overline{\boldsymbol{x}}(i) - \boldsymbol{W}(t)\overline{\boldsymbol{y}}(i)\|_2^2 \tag{44}$$

where $\overline{\boldsymbol{y}}(i) \approx \boldsymbol{W}^T(i-1)\overline{\boldsymbol{x}}(i)$ is the projection approximation. The subspace $\boldsymbol{W}(t)$ in (44) can be recursively solved using the robust PAST algorithm in [32], which is based on the robust recursive least M-estimate algorithm [22]. Additional reorthonormalization as in OPAST can also be performed, which yields the proposed R-OPASTd and R-OPASTr as shown in Tables II and III, respectively. We can see from the table that the conventional PAST algorithm is invoked to update $\boldsymbol{W}(t)$ followed by the reorthonormalization. If necessary, the

TABLE IV
ARITHMETIC COMPLEXITY OF DIFFERENT ALGORITHMS UNDER DIFFERENT DETECTION CRITERIA

Detection criteria	Number of eigenvalues required	Arithmetic Complexity of different algorithms				
		Proposed approaches		Conventional approaches		
		R-OPASTr	R-OPASTd	PCA	EWM-PCA	R-PCA
Proposed robust detection criteria						
Robust SPE	Not required	$4PB+O(B^2)$	$4PB+O(B^2)$	$O(P^3)$	$O(P^3)$	$O(P^3)$
Robust T^2 score	B	$4PB+O(B^3)$	$4PB+O(B^2)$	$O(P^3)$	$O(P^3)$	$O(P^3)$
Robust SPE + Robust T^2 score	B	$4PB+O(B^3)$	$4PB+O(B^2)$	$O(P^3)$	$O(P^3)$	$O(P^3)$
Conventional detection criteria						
SPE	P	$O(P^3)$	$O(P^3)$	$O(P^3)$	$O(P^3)$	$O(P^3)$
T^2 score	B	$4PB+O(B^3)$	$4PB+O(B^2)$	$O(P^3)$	$O(P^3)$	$O(P^3)$
SPE + T^2 score	P	$O(P^3)$	$O(P^3)$	$O(P^3)$	$O(P^3)$	$O(P^3)$

eigenvectors and eigenvalues in the subspace can be computed from $\boldsymbol{U}_B(t)$ and $\boldsymbol{\Lambda}_B(t)$. In the recursive fault detection step, the desired robust scores, such as the robust SPE, robust T^2 score, etc., are computed, and the adaptive threshold (ATS) defined in (42) and (43) for the given $\psi(\overline{\boldsymbol{x}}(t))$ is used to update the detection threshold. Finally, the robust subspace is updated. If $\psi(\overline{\boldsymbol{x}}(t))=1$, normal update is performed, and the $\boldsymbol{W}(t)$, $\boldsymbol{U}_B(t)$, and $\boldsymbol{\Lambda}_B(t)$ computed in the first step of the iteration are retained. However, if $\psi(\overline{\boldsymbol{x}}(t))=0$, then a faulty sample is detected, and the quantities computed at the last iteration, i.e., $\boldsymbol{W}(t-1)$, $\boldsymbol{U}_B(t-1)$, and $\boldsymbol{\Lambda}_B(t-1)$, are retained. In the R-OPASTd algorithm, the eigenvalues and eigenvectors in the subspace are computed successively using the PASTd algorithm, whereas the R-OPASTr computes them recursively using the R-PCA algorithm.

Table IV summarizes the arithmetic complexity of the various algorithms using the proposed robust detection criteria and conventional detection criteria. Generally, the R-OPASTr and the R-OPASTd offer lower complexity than other algorithms. If the robust T^2 score is used, the arithmetic complexities are $4PB+O(B^3)$ and $4PB+O(B^2)$ flops per iteration for R-OPASTr and R-OPASTd, respectively, which are much lower than $O(P^3)$ flops per iteration required by the PCA, EWM-PCA, and R-PCA. Moreover, if only the robust SPE is used, the arithmetic complexity for R-OPASTr and R-OPASTd can be further reduced to $4PB+O(B^2)$ flops per iteration [18] because the computation of eigenvectors and eigenvalues is not required. If both the robust SPE and robust T^2 score are used for the two algorithms, the complexity is $4PB+O(B^3)$ because both the major eigenvectors and the eigenvalues are computed.

IV. SIMULATION RESULTS

In this section, we consider a local fault or outlier detection problem and compare the proposed subspace-based algorithms with other conventional algorithms, namely, the PCA-based algorithm in [9], EWM-PCA in [12], and R-PCA in [14]. Note that, after the faulty sample is identified, its subsequent effect can be estimated and may need to be compensated to facilitate the following detection [8]. In the following simulation, we focus on the fault detection part. Regarding the additional option of the fault replacement, interested readers are referred to [8] for more details. As an illustration, we employ a real data set obtained from the Intel Laboratory [39]. The data set that we tested was collected on February 28, 2004 from one sensor node, and it consists of 1317 samples without any missing data. For each sample, there are four measurement variables: temperature, humidity, light intensity, and voltage.

In the data set, since the variables are in different physical units, scaling is required to avoid variables with larger scales dominating the shape of the estimated PCs/signal subspace due to their higher variance [28], [29]. Therefore, data preprocessing is carried out to scale all variables to unit variance. First, the background variance is estimated from the whole data set. Then, scaling is performed by dividing each measurement vector with the standard deviation obtained. After scaling the data set, the background variance of the data set is $\sigma_s^2=1$. To study the performance of the proposed approach and other approaches, we insert simulated faults in the form of impulsive outliers randomly in the data set. The impulsive outliers are generated using the contaminated Gaussian model as follows: [23]

$$\boldsymbol{n}(t)\sim(1-\eta)N\left(\boldsymbol{0},\sigma_g^2\boldsymbol{I}\right)+\eta N\left(\boldsymbol{0},\sigma_{\mathrm{im}}^2\boldsymbol{I}\right) \tag{45}$$

where $\boldsymbol{n}(t)$ is the impulsive outlier injected into the data set at time instant t, η is the occurrence probability of impulsive outlier, and $N(\boldsymbol{\mu},\boldsymbol{R})$ denotes a multivariate Gaussian distribution with mean $\boldsymbol{\mu}$ and covariance $\boldsymbol{R}$. σ_{im}^2 is the variance of the impulsive component, and σ_g^2 is the variance of the additive Gaussian component. As an illustration, η and σ_g^2 are chosen as 0.1 and 1, respectively. Hence, the probability of impulsive fault occurrence is 0.1, which is sufficiently large to evaluate the reliability of the system. The impulse-to-noise ratio (INR) σ_{dB}, which is the ratio of the impulsive noise variance σ_{im}^2 to the background variance σ_s^2 in decibels, is given by

$$\sigma_{\mathrm{dB}}=10\log_{10}\left(\frac{\sigma_{\mathrm{im}}^2}{\sigma_{\mathrm{s}}^2}\right). \tag{46}$$

It measures the strength of the impulsive noise over the background noise. The forgetting factors and window lengths in (13) and (33)–(36) are chosen as 0.99 and 11, respectively. The number of chosen PCs and the dimension of the signal subspace is $B=1$, which are determined by Kaiser's rule. An initial data block of length 11, i.e., from $t=0$ to $t=10$, is used to initialize all algorithms for later recursive update except the PCA, which works on the whole data set. The three detection criteria mentioned in Section II are used for the conventional

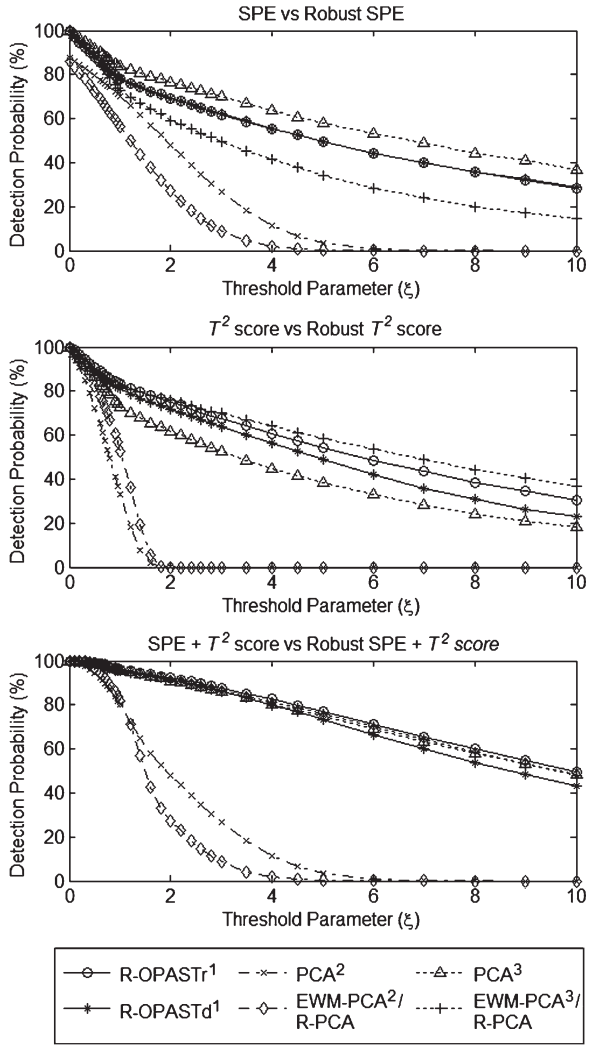

Fig. 1. DP (in percent) for different threshold parameters (ξ) of various approaches under $B = 1$ and $\sigma_{\rm dB} = 10$ dB. [1]Proposed approaches. [2]Conventional approaches. [3]Other approaches using the proposed robust detection criteria. Similar remarks also apply to Figs. 2–4.

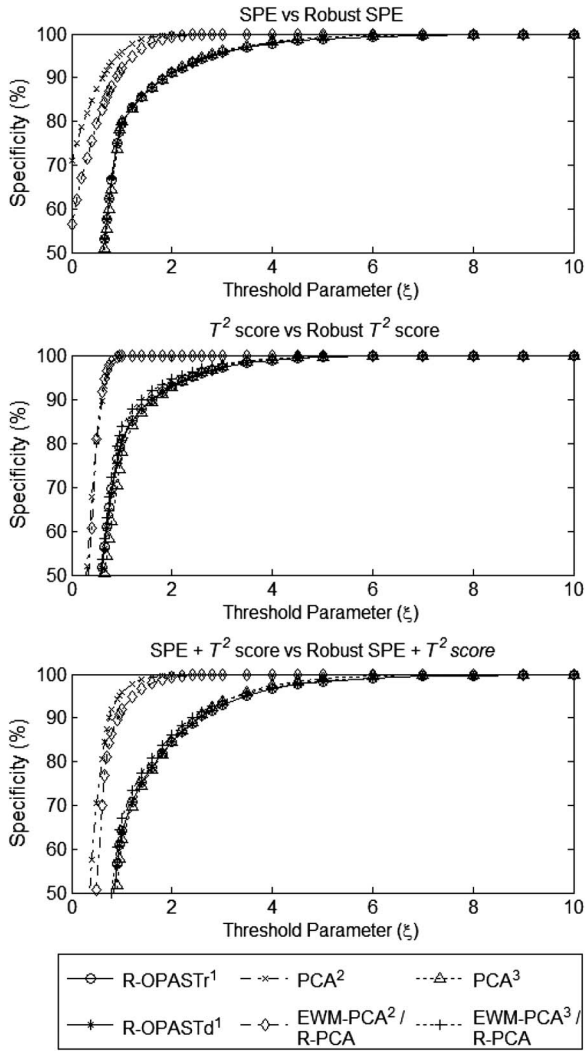

Fig. 2. Standard deviation of AUC ($\sigma_{\rm AUC}$) of various approaches for $B = 1$. [1,2,3]See remarks in Fig. 1.

algorithms. For the proposed algorithms, similar criteria are derived using the proposed robust T^2 score and robust SPE, and they are referred to as the robust detection criteria in later sections. The performance of all algorithms is assessed by the following measures, namely, detection probability (DP) and specificity:

$$DP = \frac{TP}{TP + FN} \tag{47}$$

$$Specificity = \frac{TN}{TN + FP} \tag{48}$$

where TP is the number of true positives, FN is the number of false negatives, TN is the number of true negatives, and FP is the number of false positives. The DP and specificity are both important in evaluating the performance of an algorithm. The proportion of true positives and negatives in real data may not be equal in many situations. The DP gives a better description of the algorithm when the proportion of TP is more than TN and vice versa for the specificity. The DP and specificity are calculated by averaging the results obtained in 500 Monte Carlo simulations.

A. Comparison Between the Proposed and Conventional Approaches

We compare the performance between the proposed R-OPASTr and R-OPASTd algorithms with the conventional approaches. Figs. 1 and 2 show the DP (in percent) and specificity (in percent) of the different approaches for the threshold parameter $\xi \in [0, 10]$, which correspond to a detection confidence interval of 0% and approximately 100%, i.e., $P(-\xi \leq X < \xi) \to 1$, respectively. For each ξ, ξ_F for the conventional T^2 score-based detection criterion in (9) is calculated using (11). We can see that the proposed approaches generally show higher DP than the conventional approaches at the expense of lower specificity. Also, different approaches obtain their optimal DP and specificity at different ξ.

In order to assess the general performance of the algorithms, the area under the receiver operating characteristic curve (AUC) is commonly used, and it describes the area formed by TP–FP pairs obtained from different ξ. More precisely, it can be obtained by the trapezoidal rule as follows [40]:

$$AUC = \frac{1}{2N_1N_2} \sum_{i=1}^{K} (FP_{i+1} - FP_i)(TP_{i+1} + TP_i) \tag{49}$$

TABLE V
AUC'S FOR DIFFERENT APPROACHES USING DIFFERENT DETECTION CRITERIA FOR $B = 1$ AND $\sigma_{\rm dB} = 10$ dB

	Proposed Approaches		Conventional Approaches		Other approaches using the proposed robust detection measures	
	R-OPASTr	R-OPASTd	PCA	EWM-PCA / R-PCA	PCA	EWM-PCA / R-PCA
	Robust SPE		SPE		Robust SPE	
μ_{AUC}	0.9081	0.9079	0.2121	0.3270	0.9310	0.9025
σ_{AUC}	0.0056	0.0056	0.0162	0.0935	0.0049	0.0075
	Robust T^2 score		T^2 score		Robust T^2 score	
μ_{AUC}	0.7775	0.7781	0.6487	0.7650	0.6580	0.7559
σ_{AUC}	0.0093	0.0095	0.0106	0.0100	0.0088	0.0094
	Robust SPE + Robust T^2 score		SPE + T^2 score		Robust SPE + Robust T^2 score	
μ_{AUC}	0.9481	0.9475	0.9304	0.9436	0.9401	0.9459
σ_{AUC}	0.0039	0.0037	0.0056	0.0060	0.0040	0.0042

where TP_i and FP_i, $i = 1, 2, \ldots, K$, are the corresponding TP and FP for the ith chosen $\xi \in [0, 10]$. N_1 and N_2 are the numbers of normal samples and impulsive outliers, respectively. The best possible AUC for an algorithm is 1.0, which yields 100% DP and specificity. An acceptable algorithm must have an AUC greater than 0.5 in order to yield performance better than random guessing. To quantify the performance of the algorithms, we obtained the mean AUC and standard deviation of AUC over 500 Monte Carlo simulations, and they are denoted by $\mu_{\rm AUC}$ and $\sigma_{\rm AUC}$, respectively. Table V shows the AUC of various algorithms under different detection criteria with $\sigma_{\rm dB} = 10$ dB and $B = 1$. We can see that, for SPE-based detection criterion and $SPE + T^2$ score-based detection criterion, the performance of the proposed algorithms (columns 2 and 3) is better than other conventional algorithms (columns 4–6) because they have larger $\mu_{\rm AUC}$ and smaller $\sigma_{\rm AUC}$. In particular, $\mu_{\rm AUC}$'s of the proposed algorithms are about three times larger than those of the conventional algorithms for SPE-based detection criterion. On the other hand, for T^2-based detection, $\mu_{\rm AUC}$'s of the proposed algorithms are nearly identical to other conventional algorithms except for the PCA. However, $\sigma_{\rm AUC}$'s of the proposed approaches are much lower than all conventional algorithms.

The proposed R-OPASTr and R-OPASTd algorithms generally perform better than the conventional algorithms because of the following two reasons.

1) The robust subspace tracking efficiently removes the outliers from the data set, which reduces the adverse effect of outliers on the estimated subspace.
2) The robust and adaptive nature of the proposed detection criteria improves the reliability of choosing an appropriate detection threshold and, thus, improves detection accuracy.

Moreover, we note that the required complexities for the proposed algorithms are much lower, as illustrated in Table IV.

B. Comparison Between Different Detection Criteria

In this example, the usefulness of the proposed robust detection criteria is studied. By incorporating them into the conventional algorithms, the performances of the conventional algorithms are greatly improved, as shown in columns 7–9 of Table V. In particular, $\mu_{\rm AUC}$ for robust SPE-based detection criterion (columns 7–9) is about three times larger than that for the conventional SPE-based detection criterion (columns 4–6), at the expense of the slight decrease in $\mu_{\rm AUC}$ for the robust T^2 score counterpart. However, $\sigma_{\rm AUC}$ is still smaller for both robust criteria. Also, for the robust SPE $+ T^2$ score-based detection criteria, larger $\mu_{\rm AUC}$ and smaller $\sigma_{\rm AUC}$ are observed.

The robust SPE offers improvement over the conventional SPE because of its robustness against the undesired outliers. On the other hand, the cubic term in the conventional SPE detection threshold in (8) magnifies the effect of the outliers on the eigenvalues, and this contributes to the deteriorated performance when using the conventional SPE.

Nevertheless, we can see from Table IV that the complexity of the conventional algorithms using the proposed robust detection criteria remains at $O(P^3)$ because the complexity is still dominated by the computation of all eigenvalues. Unlike the conventional algorithms, the proposed algorithms effectively eliminate the need of computing the unused eigenvalues, and hence, they have the lowest complexity among others.

C. Effect of the INR

In this example, we study the effect of INR $\sigma_{\rm dB}$ on the performance of various algorithms by varying $\sigma_{\rm dB}$ from 8 to 20 dB. As can be seen in Figs. 3 and 4, most algorithms generally have larger $\mu_{\rm AUC}$ and smaller $\sigma_{\rm AUC}$ as $\sigma_{\rm dB}$ increases. This is expected because impulses with larger amplitudes are more likely to be correctly identified. However, an increasing $\sigma_{\rm dB}$ significantly degrades the performance of the conventional algorithms using the SPE-based detection criterion, in which the threshold is very sensitive to the accuracy of eigenvalues estimated. Therefore, the fault detection is more likely to break down due to the great influence of impulsive outliers with larger amplitudes on the eigenvalues.

Overall, the proposed R-OPASTr and R-OPASTd algorithms perform better than other conventional algorithms when $\sigma_{\rm dB}$

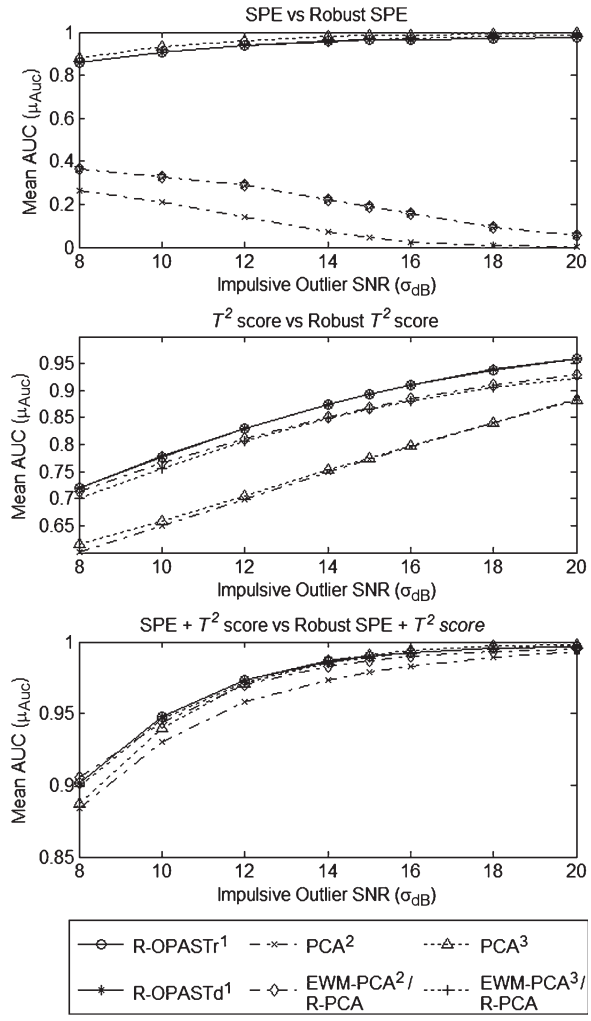

Fig. 3. Mean AUC (μ_{AUC}) of various approaches for $B = 1$. [1,2,3]See remarks in Fig. 1.

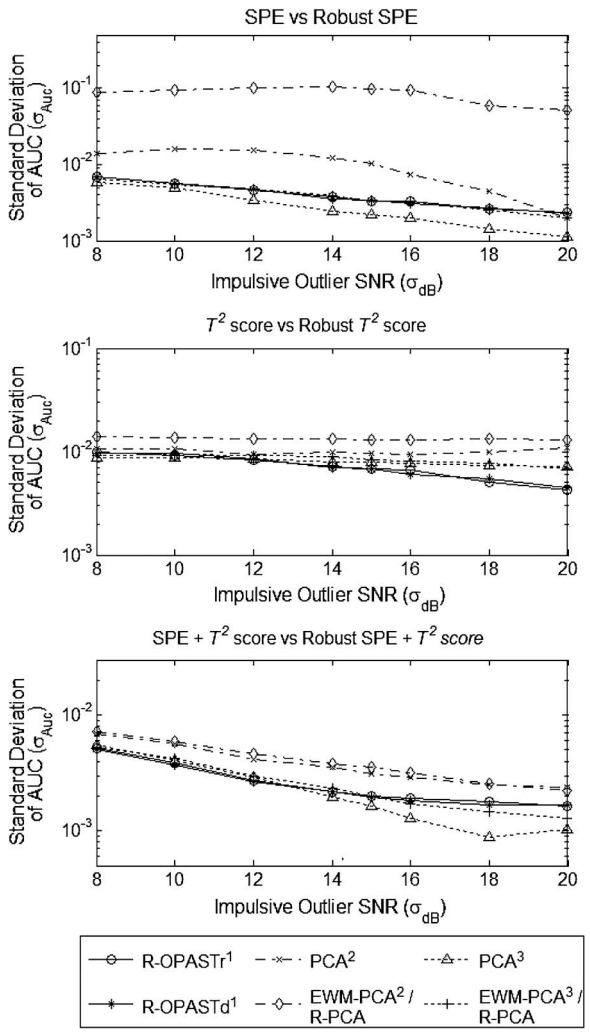

Fig. 4. Standard deviation of AUC (σ_{AUC}) of various approaches for $B = 1$. [1,2,3]See remarks in Fig. 1.

increases. Moreover, we can see that the proposed robust detection criteria offer improvement to the performance of these conventional algorithms.

D. Effect of the Subspace Dimension B

In this example, we study how the subspace dimension affects the performance of various algorithms. The simulation settings are the same as before, except that the subspace dimension is chosen as $B = 2$ according to MDL, and the results are shown in Table VI. It can be seen from Tables V and VI that the performance improvement of the R-OPASTr algorithm is more pronounced than the R-OPASTd algorithm when the subspace dimension increases. This is mainly attributed to the fact that the R-OPASTd algorithm suffers from performance degradation due to the loss of orthonormality of the eigenvectors caused by the relaxation made on the loss function in (15). Consequently, the accuracy of the R-OPASTd algorithm in computing the eigenvalues and the resultant subspace is not as good as that of the R-OPASTr algorithm. This suggests that the proposed eigenvector and eigenvalue computation approach contributes to the better performance of R-OPASTr. On the other hand, the deflation approach has a lower arithmetic complexity at the expense of some performance degradation.

V. Experimental Validation Using Real WSN Data Set

In this section, we present a realistic example where the proposed methods are used to detect anomalies observed in real WSN data. For illustration purposes, we analyze a real WSN data set collected from the Networked Aquatic Microbial Observing System (NAMOS) [41]. The NAMOS is a collaborative research project involving robotics, sensor networks, and marine biology. It has deployed sensor networks at different locations to facilitate real-time observation of aquatic ecosystems and sensor-actuated sampling for biological analysis. In particular, we consider the WSN data collected at James Reserve (Lake Fulmor, Mountain Center, CA 92561, USA) during the time interval from August 28, 2006 to September 1, 2006. The data consist of ten variables (six temperature readings, chlorophyll reading, light intensity, wind speed, and wind direction). Fig. 5 shows the ten readings recorded by sensor nodes 102 and 103. We can see that three extreme constant levels are observed in the chlorophyll reading of node 103, which deviates considerably from that of node 102. At the end of the record, we can also observe a sudden change of chlorophyll and thermister

TABLE VI
AUC'S FOR DIFFERENT APPROACHES USING DIFFERENT DETECTION CRITERIA FOR $B = 2$ AND $\sigma_{\mathrm{dB}} = 10$ dB

	Proposed Approaches		Conventional Approaches		Other approaches using the proposed robust detection measures	
	R-OPASTr	R-OPASTd	PCA	EWM-PCA / R-PCA	PCA	EWM-PCA / R-PCA
	Robust SPE		SPE		Robust SPE	
μ_{AUC}	0.8393	0.8385	0.2270	0.2975	0.8833	0.8110
σ_{AUC}	0.0072	0.0070	0.0168	0.0562	0.0058	0.0091
	Robust T^2 score		T^2 score		Robust T^2 score	
μ_{AUC}	0.8821	0.8706	0.8309	0.8874	0.8136	0.8672
σ_{AUC}	0.0063	0.0064	0.0112	0.0096	0.0072	0.0069
	Robust SPE + Robust T^2 score		SPE + T^2 score		Robust SPE + Robust T^2 score	
μ_{AUC}	0.9531	0.9481	0.9466	0.9304	0.9493	0.9479
σ_{AUC}	0.0037	0.0038	0.0052	0.0061	0.0036	0.0041

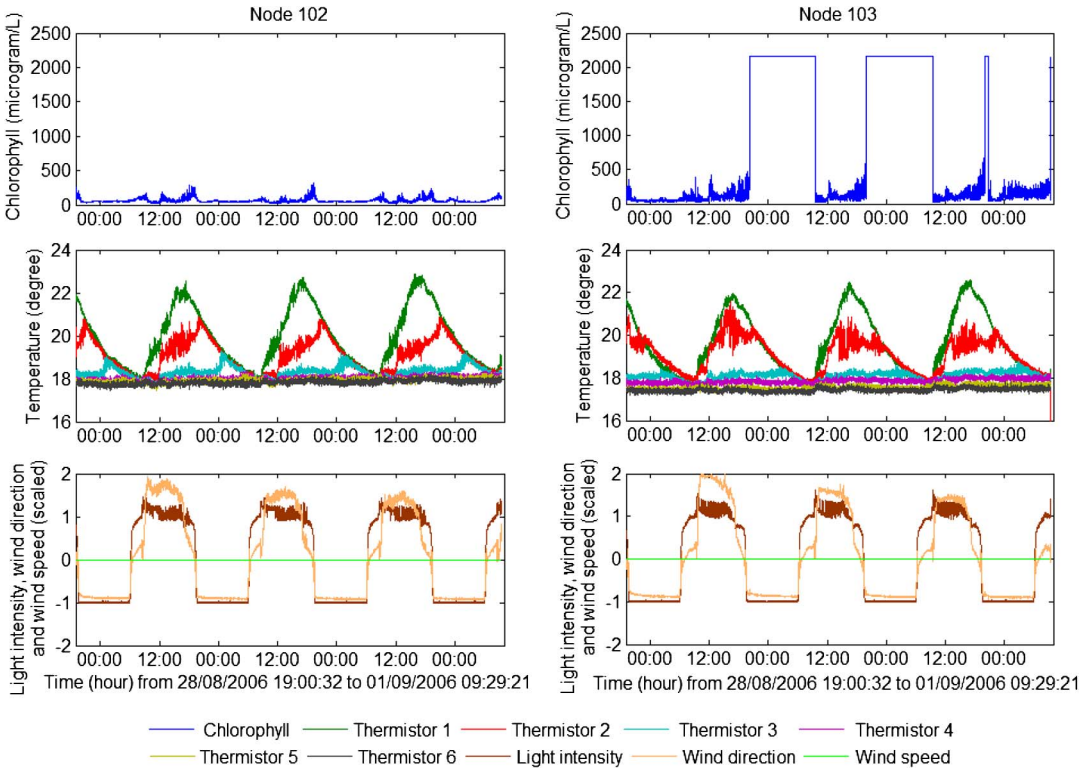

Fig. 5. Chlorophyll, temperature, light intensity, and wind speed and direction readings recorded by sensor nodes (left) 102 and (right) 103 at James Reserve (Lake Fulmor), during the time interval from August 28, 2006 to September 1, 2006. For better visibility, the light intensity and wind direction and speed readings are centered (mean removed) and scaled.

2 readings. According to [25] and [42], such abnormal readings are possibly caused by sensor malfunction, unstable wireless connection, or packet collisions. Since these constant abnormal readings or sudden change can be treated similarly as the mean-shift faults, they can also be detected by the proposed fault detection algorithms in the wavelet domain, as mentioned in Section II.

It is well known that the DWT of a discrete-time signal can be efficiently computed using a tree-structure analysis filterbank, which contains a set of two-channel analysis filterbanks [43], [44]. Suppose that the reading of the pth variable at time t is

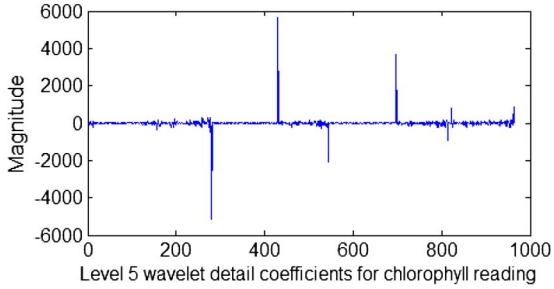

Fig. 6. Level-5 wavelet detail coefficients for the chlorophyll reading of node 103 shown in Fig. 5.

TABLE VII
SUMMARY OF ABNORMAL READINGS AND CORRESPONDING WAVELET COEFFICIENTS

Time	Event	Wavelet Coeff.
29/08/2006 20:06	Start of abnormal chlorophyll reading	280
30/08/2006 09:14	End of abnormal chlorophyll reading	430
30/08/2006 19:50	Start of abnormal chlorophyll reading	544
31/08/2006 09:32	End of abnormal chlorophyll reading	697
31/08/2006 20:01	Start of abnormal chlorophyll reading	814
31/08/2006 20:44	End of abnormal chlorophyll reading	822
01/09/2006 09:24	Abrupt change in chlorophyll and thermister 2 readings	963

TABLE VIII
AUC'S OF DIFFERENT APPROACHES FOR NAMOS DATA SET [41]

	Proposed Approaches		Conventional Approaches		Other approaches using the proposed robust detection measures	
	R-OPASTr	R-OPASTd	PCA	EWM-PCA / R-PCA	PCA	EWM-PCA / R-PCA
	Robust SPE + Robust T^2 score		SPE + T^2 score		Robust SPE + Robust T^2 score	
AUC	0.9859	0.9736	0.9231	0.9574	0.9618	0.9778

denoted by $x_p(t)$. Then, its wavelet approximation and detail coefficients at level γ can be computed, respectively, as

$$a_p^{(\gamma)}(t) = \sum_{n=-\infty}^{\infty} h(n) a_p^{(\gamma-1)}(2t-n)$$
$$d_p^{(\gamma)}(t) = \sum_{n=-\infty}^{\infty} g(n) a_p^{(\gamma)}(2t-n) \quad (50)$$

where $a_p^{(0)}(t) = x_p(t)$ and $h(n)$ and $g(n)$ are the impulse responses of the low-pass and high-pass filters of the two-channel analysis filterbanks, respectively. For simplicity, we employed the Haar wavelet with $h(0) = h(1) = g(1) = 1/\sqrt{2}$ and $g(0) = -1/\sqrt{2}$ to transform the measurements of all ten variables. Fig. 6 shows the level-5 wavelet detail coefficients of the chlorophyll readings at node 103 which exhibits obvious abnormality. However, the details of other readings are omitted due to page limitation. As expected, we can see from Fig. 6 that the sudden rise (fall) of the readings results in negative (positive) impulse in the wavelet domain. Tables VII summarizes the wavelet coefficients associated with the occurrence of abnormal chlorophyll readings observed at node 103.

For each variable, the first 250 level-5 wavelet detail coefficients are used as the training data, while the remaining coefficients are used as the testing data after scaling by the standard deviation of the training data. Similar to Section IV, we carry out the comparison of the proposed algorithms with other PCA-based algorithms using identical experimental procedures and settings, i.e., the forgetting factors, window lengths, and threshold parameter are chosen as 0.99, 11, and $\xi \in [0, 10]$, respectively. According to Kaiser's rule, the number of chosen PCs (or subspace dimension) is determined to be $B = 5$. Tables VIII shows the AUC's of different algorithms based on either $SPE + T^2$ score-based detection criterion or its robust counterpart. We can see that both the proposed R-OPASTr and R-OPASTd outperform the PCA-based algorithms. Moreover, the proposed robust detection criterion generally improves the performance of the PCA-based algorithms. Similar findings can be obtained for other detection criteria in general, but they are omitted due to page limitation.

VI. CONCLUSION

New robust recursive ED and subspace-based algorithms for fault detection in WSNs and related applications have been proposed. The major advantages of algorithms developed under the proposed approach are the following: 1) it computes recursively the ED in the major subspace with a smaller dimension and, therefore, facilitates online implementation with reduced arithmetic complexity and improved adaptability to gradual system change; 2) it has two different ways to update the ED required, namely, R-OPASTr and R-OPASTd, which offer different tradeoffs between fault detection accuracy and implementation complexity; and 3) it incorporates robust statistics in the ED update, and hence, its capability to detect faulty samples is improved. Together with the proposed robust detection criteria and their efficient recursive implementation, it is shown through simulation and experimental results that the proposed approach generally outperforms other PCA-based approaches in both detection accuracy and implementation complexity. The algorithms developed in this paper may also find applications in process monitoring and other related applications.

REFERENCES

[1] N. Ramanathan, L. Balzano, M. Burt, D. Estrin, E. Kohler, T. Harmon, C. Harvey, J. Jay, S. Rothenberg, and M. Srivastava, "Rapid deployment with confidence: Calibration and fault detection in environmental sensor networks," Center Embedded Netw. Sens., Los Angeles, CA, Tech. Rep. 62, Apr. 2006.

[2] A. Tiwari, P. Ballal, and F. Lewis, "Energy-efficient wireless sensor network design and implementation for condition-based maintenance," *ACM Trans. Sens. Netw.*, vol. 3, no. 1, p. 1, Mar. 2007.

[3] K. Yunseop, R. G. Evans, and W. M. Iversen, "Remote sensing and control of an irrigation system using a distributed wireless sensor network," *IEEE Trans. Instrum. Meas.*, vol. 57, no. 7, pp. 1379–1387, Jul. 2008.

[4] F. Salvadori, M. de Campos, P. S. Sausen, R. F. de Camargo, C. Gehrke, C. Rech, M. A. Spohn, and A. C. Oliveira, "Monitoring in

industrial systems using wireless sensor network with dynamic power management," *IEEE Trans. Instrum. Meas.*, vol. 58, no. 9, pp. 3104–3111, Sep. 2009.
[5] Z. Yang, N. Meratnia, and P. Havinga, "Outlier detection techniques for wireless sensor networks: A survey," *IEEE Commun. Surveys Tuts.*, vol. 12, no. 2, pp. 159–170, Second Quarter, 2010.
[6] G. Tolle, J. Polastre, R. Szewczyk, D. Culler, N. Turner, K. Tu, S. Burgess, T. Dawson, P. Buonadonna, D. Gay, and W. Hong, "A macroscope in the redwoods," in *Proc. 3rd Int. Conf. Embedded Netw. Sens. Syst.*, 2005, pp. 51–63.
[7] B. Sheng, Q. Li, W. Mao, and W. Jin, "Outlier detection in sensor networks," in *Proc. ACM MobiHoc*, 2007, pp. 219–228.
[8] B. M. Wise and N. L. Ricker, "Recent advances in multivariate statistical process control: Improving robustness and sensitivity," in *Proc. Int. Symp. Adv. Control Chem. Process.*, 1991, pp. 125–130.
[9] V. Chatzigiannakis, S. Papavassiliou, M. Grammatikou, and B. Maglaris, "Hierarchical anomaly detection in distributed large-scale sensor networks," in *Proc. IEEE ISCC*, Sep. 2006, pp. 761–767.
[10] A. Maghsooloo, A. Khosrvai, H. S. Anvar, and R. Barzamini, "ANFIS and PCA capability assessment for fault detection in unknown nonlinear systems," in *Proc. IEEE ISCCSP*, Mar. 2008, pp. 47–52.
[11] V. Chatzigiannakis and S. Papavassiliou, "Diagnosing anomalies and identifying faulty nodes in sensor networks," *IEEE Sens. J.*, vol. 7, no. 5, pp. 637–645, May 2007.
[12] D. X. Tien, K. W. Lim, and L. Jun, "Comparative study of PCA approaches in process monitoring and fault detection," in *Proc. IECON*, May 2004, vol. 3, pp. 2594–2599.
[13] S. Lane, E. Martin, A. Morris, and P. Gower, "Application of exponentially weighted principal component analysis for the monitoring of a polymer film manufacturing process," *Trans. Inst. Meas. Control*, vol. 25, no. 1, pp. 17–35, Mar. 2003.
[14] W. Li, H. Yue, S. Valle-Cervantes, and S. Qin, "Recursive PCA for adaptive process monitoring," *J. Process Control*, vol. 10, no. 5, pp. 471–486, Aug. 2000.
[15] R. D. DeGroat, "Noniterative subspace tracking," *IEEE Trans Signal Process.*, vol. 40, no. 3, pp. 571–577, Mar. 1992.
[16] N. Owsley, "Adaptive data orthogonalization," in *Proc. IEEE ICASSP*, Apr. 1978, vol. 3, pp. 109–112.
[17] B. Yang, "Projection approximation subspace tracking," *IEEE Trans. Signal Process.*, vol. 43, no. 1, pp. 95–107, Jan. 1995.
[18] K. Abed-Meraim, A. Chkeif, Y. Hua, and T. Paris, "Fast orthonormal PAST algorithm," *IEEE Signal Process. Lett.*, vol. 7, no. 3, pp. 60–62, Mar. 2000.
[19] T. Gustafsson, "Instrumental variable subspace tracking using projection approximation," *IEEE Trans. Signal Process.*, vol. 46, no. 3, pp. 669–681, Mar. 1998.
[20] X. Li and H. Fan, "Blind channel identification: Subspace tracking method without rank estimation," *IEEE Trans. Signal Process.*, vol. 49, no. 10, pp. 2372–2382, Oct. 2001.
[21] A. Chkeif, K. Abed-Meraim, G. Kawas-Kaleh, and Y. Hua, "Spatio-temporal blind adaptive multiuser detection," *IEEE Trans. Commun.*, vol. 48, no. 5, pp. 729–732, May 2000.
[22] S. C. Chan and Y. Zou, "A recursive least M-estimate algorithm for robust adaptive filtering in impulsive noise: Fast algorithm and convergence performance analysis," *IEEE Trans. Signal Process.*, vol. 52, no. 4, pp. 975–991, Nov. 2004.
[23] P. J. Huber, *Robust Statistics*. New York: Wiley, 1981.
[24] M. Daszykowski, K. Kaczmarek, I. Stanimirova, Y. Vander Heyden, and B. Walczak, "Robust SIMCA-bounding influence of outliers," *Chemometrics Intell. Lab. Syst.*, vol. 87, no. 1, pp. 95–103, May 2007.
[25] Y. Y. Li and L. E. Parker, "Classification with missing data in a wireless sensor network," in *Proc. IEEE Southeastcon*, Apr. 2008, pp. 533–538.
[26] S. Mallat and W. L. Hwang, "Singularity detection and processing with wavelets," *IEEE Trans. Inf. Theory*, vol. 38, no. 2, pp. 617–643, Mar. 1992.
[27] B. Bakshi, "Multiscale PCA with application to multivariate statistical process monitoring," *AIChE J.*, vol. 44, no. 7, pp. 1596–1610, Jul. 1998.
[28] J. Jackson, *A User's Guide to Principal Components*. New York: Wiley-Interscience, 1991.
[29] J. Jackson and G. Mudholkar, "Control procedures for residuals associated with principal component analysis," *Technometrics*, vol. 21, no. 3, pp. 341–349, Aug. 1979.
[30] P. F. Odgaard, L. Bao, and S. B. Jorgensen, "Observer and data-driven-model-based fault detection in power plant coal mills," *IEEE Trans. Energy Convers.*, vol. 23, no. 2, pp. 659–668, Jun. 2008.
[31] S. J. Qin, "Statistical process monitoring: Basics and beyond," *J. Chemometrics*, vol. 17, no. 8/9, pp. 480–502, Aug./Sep. 2003.
[32] S. C. Chan, Y. Wen, and K. L. Ho, "A robust PAST algorithm for subspace tracking in impulsive noise," *IEEE Trans. Signal Process.*, vol. 54, no. 1, pp. 105–116, Jan. 2006.
[33] W.K. Pratt, *Digital Image Processing*, 2nd ed. Hoboken, NJ: Wiley, 1991.
[34] H. Kaiser, "The application of electronic computers to factor analysis," *Educ. Psychol. Meas.*, vol. 20, no. 1, pp. 141–151, Apr. 1960.
[35] A. Barron, J. Rissanen, and B. Yu, "The minimum description length principle in coding and modeling," *IEEE Trans. Inf. Theory*, vol. 44, no. 6, pp. 2743–2760, Oct. 1998.
[36] G. H. Golub and C. F. Van Loan, *Matrix Computations*, 3rd ed. Baltimore, MD: Johns Hopkins Univ. Press, 1996.
[37] J. Bunch, C. Nielsen, and D. Sorensen, "Rank-one modification of the symmetric eigenproblem," *Numer. Math.*, vol. 31, no. 1, pp. 31–48, Mar. 1978.
[38] S. C. Chan and Y. Zhou, "On the performance analysis of the least mean M-estimate and normalized least mean M-estimate algorithms with Gaussian inputs and additive Gaussian and contaminated Gaussian noises," *J. Signal Process. Syst.*, vol. 60, no. 1, pp. 81–103, Jul. 2010.
[39] The Intel Lab, Berkeley data set, 2004. [Online]. Available: http://db.lcs.mit.edu/labdata/labdata.html
[40] T. Fawcett, "An introduction to ROC analysis," *Pattern Recognit. Lett.*, vol. 27, no. 8, pp. 861–874, Jun. 2006.
[41] NAMOS: Networked Aquatic Microbial Observing System, 2002. [Online]. Available: http://robotics.usc.edu/namos
[42] Y. Y. Li and L. Parker, "Intruder detection using a wireless sensor network with an intelligent mobile robot response," in *Proc. IEEE Southeastcon*, 2008, pp. 37–42.
[43] S. G. Mallat, "A theory for multiresolution signal decomposition: The wavelet representation," *IEEE Trans. Pattern Anal. Mach. Intell.*, vol. 11, no. 7, pp. 674–693, Jul. 1989.
[44] M. J. Shensa, "The discrete wavelet transform: Wedding the a trous and Mallat algorithms," *IEEE Trans Signal Process.*, vol. 40, no. 10, pp. 2464–2482, Oct. 1992.

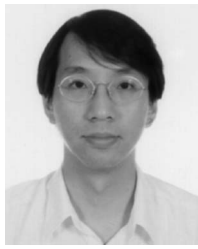

S. C. Chan (S'87–M'92) received the B.Sc.(Eng.) and Ph.D. degrees from The University of Hong Kong, Pokfulam, Hong Kong, in 1986 and 1992, respectively.

Since 1994, he has been with the Department of Electrical and Electronic Engineering, The University of Hong Kong, where he is currently a Professor. He is an Associate Editor of the *Journal of Signal Processing Systems*. His research interests include fast transform algorithms, filter design and realization, multirate and biomedical signal processing, communications and array signal processing, high-speed A/D converter architecture, bioinformatics, and image-based rendering.

Dr. Chan is currently a member of the Digital Signal Processing Technical Committee of the IEEE Circuits and Systems Society and an Associate Editor of the IEEE TRANSACTIONS ON CIRCUITS AND SYSTEMS I in 2008–2009 and the IEEE TRANSACTIONS ON CIRCUITS AND SYSTEMS II. He was the Chairman of the IEEE Hong Kong Chapter of Signal Processing in 2000–2002 and an organizing committee member of the IEEE International Conference on Acoustics, Speech and Signal Processing 2003 and the International Conference on Image Processing 2010.

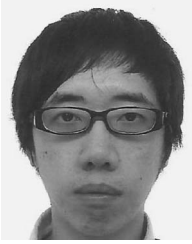

H. C. Wu received the B.Eng. degree in electric engineering from The University of New South Wales, Sydney, Australia, in 2008 and the M.Sc. degree in electrical and electronic engineering from The University of Hong Kong, Pokfulam, Hong Kong, in 2009, where he is currently working toward the Ph.D. degree in the Department of Electrical and Electronic Engineering.

His main research interests are in pattern recognition, digital signal processing, and bioinformatics.

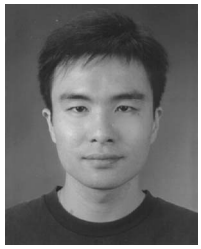

K. M. Tsui received the B.Eng., M.Phil., and Ph.D. degrees in electrical and electronic engineering from The University of Hong Kong, Pokfulam, Hong Kong, in 2001, 2004, and 2008, respectively.

He is currently a Postdoctoral Fellow with the Department of Electrical and Electronic Engineering, The University of Hong Kong. His main research interests are in array signal processing, high-speed AD converter architecture, biomedical signal processing, digital signal processing, multirate filterbank and wavelet design, and digital filter design, realization, and application.